# Nonequilibrium Energetics of a Single $F_1$-ATPase Molecule

Shoichi Toyabe,[1] Tetsuaki Okamoto,[1] Takahiro Watanabe-Nakayama,[2] Hiroshi Taketani,[1] Seishi Kudo,[3] and Eiro Muneyuki[1,*]

[1]*Faculty of Science and Engineering, Chuo University, Tokyo 112-8551, Japan*
[2]*Grad. School of Bioscience and Biotechnology, Tokyo Institute of Technology, Kanagawa 226-8503, Japan*
[3]*Faculty of Engineering, Toin University of Yokohama, Kanagawa 225-8502, Japan*

(Received 11 February 2010; published 14 May 2010)

Molecular motors drive mechanical motions utilizing the free energy liberated from chemical reactions such as ATP hydrolysis. Although it is essential to know the efficiency of this free energy transduction, it has been a challenge due to the system's microscopic scale. Here, we evaluate the single-molecule energetics of a rotary molecular motor, $F_1$-ATPase, by applying a recently derived nonequilibrium equality together with an electrorotation method. We show that the sum of the heat flow through the probe's rotational degree of freedom and the work against an external load is almost equal to the free energy change per a single ATP hydrolysis under various conditions. This implies that $F_1$-ATPase works at an efficiency of nearly 100% in a thermally fluctuating environment.

DOI: 10.1103/PhysRevLett.104.198103 PACS numbers: 87.16.Nn, 05.40.Jc, 05.70.Ln

$F_1$-ATPase, a water soluble part of $F_0F_1$-ATP syntheses, is a rotary molecular motor [1–4]. The central $\gamma$ shaft rotates unidirectionally on average within a cylinder consisting of three $\alpha$ and three $\beta$ subunits while hydrolyzing ATP to ADP and phosphate [Fig. 1(a)]. A single ATP hydrolysis triggers a 120° rotation [4,5]. By fixing an $F_1$ motor to a glass surface and attaching a probe filament or particle to the $\gamma$ shaft, we can observe its ATP-driven rotations using conventional optical microscopes at a single molecule level [3,4,6]. In cells, combined with the membrane embedded proton driven motor $F_0$, they couple ATP synthesis or hydrolysis and proton flow. Thus, $F_1$-ATPase plays a central role in biological energy transduction. Therefore, it is crucial to reveal its energetics, especially the efficiency, to understand the principle of its operation [7]. Although $F_1$-ATPase is known to be highly efficient [4], well-controlled precise evaluation has not been achieved. In this study, we evaluated the energetics of the $F_1$-ATPase by measuring thermodynamic quantities of its probe particle using a new nonequilibrium equality [8–10] together with an electrorotation method developed for torque manipulation of microscopic objects [11–13].

In single molecule experiments, what we can access is only the probe attached to molecular motors since motor proteins are quite small with a dimension of around 10 nm. Accordingly, a methodology to extract energetic information of motors from the probe motion is required. Although the probe is much larger than the motor protein, it is still sufficiently small that thermal fluctuations have a dominant effect on its behavior. The probe exchanges energy with an environment through thermal fluctuations as heat [14,15].

Consider a microscopic object moving in a viscous fluid with a frictional coefficient $\Gamma$ and a velocity $v(t)$. It feels a force of $-\Gamma v(t) + \xi(t)$ from the fluid, where $\xi(t)$ is the thermal fluctuating force. Then, the heat flow per unit time from the system to the heat bath is naturally defined as $J \equiv \langle[\Gamma v(t) - \xi(t)]v(t)\rangle$, where $\langle\cdots\rangle$ is the ensemble average [16,17]. However, since $\xi(t)$ is usually not accessible in experiments, measurement of $J$ in small fluctuating systems has been difficult. Recently, a nonequilibrium equality that enables us to calculate $J$ from experimentally accessible quantities was derived by Harada and Sasa for Langevin systems in nonequilibrium steady states [8–10] and experimentally verified [18,19]:

$$J = \Gamma v_s^2 + \Gamma \int_{-\infty}^{\infty} df[\tilde{C}(f) - 2T\tilde{R}'(f)], \qquad (1)$$

where $v_s$ is the mean velocity. $\tilde{C}(f)$ is the fluctuation of the velocity around $v_s$ calculated as the Fourier transform of the self time correlation function $C(\tau) = \langle[v(t+\tau) - v_s][v(t) - v_s]\rangle$. $\tilde{R}(f)$ is the Fourier transform of the velocity linear-response function; $\langle v(t)\rangle_N = v_s + \int_{-\infty}^{t} dsR(t-s)N(s) + O(N^2)$, where $\langle v(t)\rangle_N$ is the ensemble average of $v(t)$ under a sufficiently small probe torque $N(t)$. $\tilde{R}(f)$ indicates the sensitivity of the velocity to a perturbation

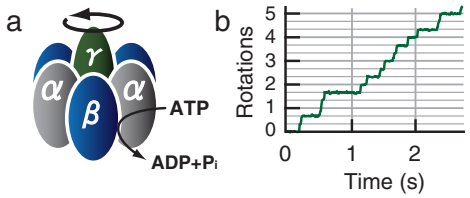


FIG. 1 (color online). (a) Schematic of $F_1$-ATPase molecule. The central $\gamma$ shaft rotates unidirectionally when ATP is hydrolyzed to ADP and phosphate. $\delta$ and $\varepsilon$ subunits are omitted for simplicity. (b) Typical trajectory at low ATP concentration (0.4 $\mu$M ATP, 0.4 $\mu$M ADP, 1 mM $P_i$). An ATP binding reaction triggers a 120° step.

 

at $f$. $\tilde{R}'(f)$ is the real part of $\tilde{R}(f)$. $T$ is the temperature. The Boltzmann constant was set to one for the briefness. Around an equilibrium state, fluctuation response relation (FRR) $\tilde{C}(f) = 2T\tilde{R}'(f)$ is known to hold [20], meaning that a system with large fluctuations is highly sensitive to an external perturbation and vice versa. On the other hand, FRR is generally violated in nonequilibrium systems [21–24]. Therefore, the magnitude of the integral in (1) indicates how far the system is from equilibrium and vanishes around the equilibrium state. Thus, the first and second terms of the equality correspond to the dissipation originating in the steady motion and that originating in the nonequilibrium fluctuations, respectively. It should be noted that heat can dissipate through multiple degrees of freedom, including rotations, swings, radial fluctuations, etc., in a rotational system such as $F_1$-ATPase. The equality enables us to track the energy flow in terms of the amount of heat dissipation through the degree of freedom that we are interested in by measuring the fluctuation and response of that degree of freedom. In the following, we focus on the rotational degree of freedom of the probe, where $v(t)$ is the rotational velocity and $\Gamma$ the rotational frictional coefficient.

The experimental setup including the torque calibration was essentially the same as that in [13] (see [25] for the details). $F_1$ molecules derived from a thermophilic *Bacillus* PS3 with mutations ($His_6 - \alpha C193S/W463F$, $His_{10} - \beta$, $\gamma S107C/I210C$) [5] were fixed on a cover slip functionalized by $Ni^{2+}$-NTA [Fig. 2(a)]. Rotations of a dimeric probe particle with a diameter of 0.287 $\mu$m attached to the $\gamma$ shaft were observed at $24 \pm 1$ °C in a buffer containing 5 m$M$ MOPS-K, indicated amount of ATP, ADP, $P_i$, and 1 m$M$ excess of $MgCl_2$ over ATP and ADP ($p$H 6.9) on a phase-contrast microscope (Olympus) equipped with a high-speed camera at 1800 Hz. Torque necessary for a constant external load and the response measurement was induced using an electrorotation method [11–13] as illustrated in Fig. 2. The magnitude of torque is proportional to the square of the amplitude of the applied voltage and the volume of the dielectric objects. For the torque calibration, we measured the torque-voltage relation of multiple freely-rotating particles in each chamber (see [25] for details). The obtained calibration curve was applied to the $F_1$-ATPase's probe particle by assuming that the torque on such freely-rotating particle and that on the $F_1$-ATPase's probe particle are similar in the same chamber. To measure the linear frequency response function, a sinusoidal torque with a sufficiently-small magnitude [25] was applied by modulating the amplitude of the induced 10 MHz AC voltage periodically at various frequencies.

At a low ATP concentration, the probe attached to the $\gamma$ shaft of $F_1$-ATPase rotated unidirectionally with discrete 120° steps (Fig. 1). Intervals between steps correspond to the waiting time for ATP binding. On the other hand, some particles showed bidirectional rotational Brownian motion. They were supposed to be attached to collapsed $F_1$ molecules or the glass surface through some nonspecific bindings. As a control, we measured $\tilde{C}(f)$ and $\tilde{R}'(f)$ of such fluctuating particles in a buffer lacking ATP, ADP, and $P_i$. Figure 3(a) shows that the FRR holds to a good extent, or $\tilde{C}(f)$ and $2T\tilde{R}'(f)$ coincide well, except in the high frequency region, where system noise, aliasing effects due to the finite sampling rate, and the finite exposure time distort the data. On the other hand, for continuously rotating particles driven by $F_1$ molecules in a buffer containing ATP, ADP, and $P_i$, the FRR was violated in the low frequency region [Fig. 3(b)]. $\tilde{C}(f)$ is supposed to be the superposition of two spectra; the high frequency region reflects Brownian motion in ATP waiting dwells, and the low frequency region reflects stepwise rotations. Then, we examined the dependence of $\tilde{C}(f)$ and $\tilde{R}'(f)$ on ATP, ADP, and $P_i$ concentrations. As ATP and ADP concentrations were simultaneously increased, average rotational velocity and both $\tilde{C}(f)$ and $\tilde{R}'(f)$ increased [Fig. 3(b)–3(d)]. At low ATP concentrations, since $F_1$-ATPase spends most of its time trapped in the ATP waiting state, the fluctuation and response are suppressed. On the other hand at high ATP concentrations, it behaves like a Brownian particle running down a potential gradient, causing the increase in $\tilde{C}(f)$ and $\tilde{R}'(f)$. When we held the ATP concentration constant and decreased the ADP and $P_i$ concentrations, the average velocity was nearly the same. In this case, although $\tilde{R}'(f)$ remained almost constant [Figs. 3(c) and 3(e)], $\tilde{C}(f)$ in-

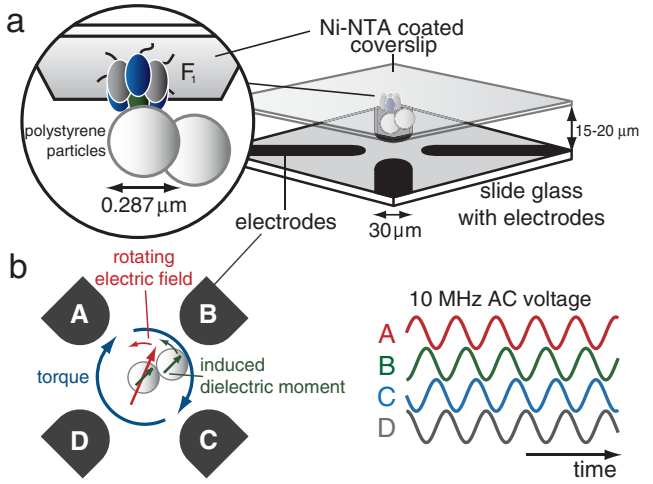


FIG. 2 (color online). (a) Experimental setup. A dimeric polystyrene particle is attached to the $\gamma$ shaft of $F_1$-ATPase fixed on the top glass surface. Four electrodes are coated on the bottom glass surface. Distance between electrodes is 50 $\mu$m. (b) Electrorotation method. A rotating electric field at a frequency of 10 MHz was generated at the center of four electrodes by applying sinusoidal voltages with a phase shift of $\pi/2$. Dielectric objects in this rotating electric field have a dielectric moment rotating at 10 MHz. The phase delay between the electric field and the dielectric moment resulted in the torque on the objects. Temperature rise due to the electric field was at most 0.3 °C, which was smaller than the temperature variance of the environment. Not to scale.

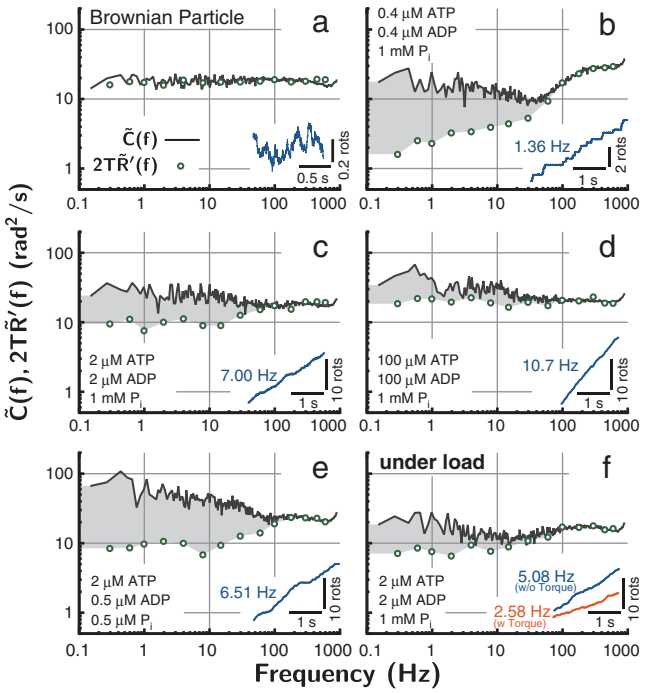


FIG. 3 (color online). Typical examples of fluctuations $\tilde{C}(f)$ (lines) and responses $2T\tilde{R}'(f)$ (circles) of the rotational velocities. The shaded area corresponds to the half of the integral in (1). The rotational trajectory is shown in the inset. rots: rotations. (a) Rotational Brownian particle in the absence of ATP, ADP, and $P_i$. (b)–(f) Particles driven by $F_1$-ATPase at indicated concentrations of substrates. (f) Under an external load of 17.7 pN nm/rad.

creased significantly. This is probably due to the change of fluctuations triggered by the binding and release of ADP and $P_i$, while an apparent difference in the rotational behavior was not evident. At last, we imposed a constant external load in the opposing direction of the ATP-driven rotations. A torque of 17.7 pN nm/rad decreased the mean rotational velocity of a probe from 5.08 Hz to 2.58 Hz [Fig. 3(f)]. Under such an opposing torque, the extent of FRR violation, or the discrepancy between $\tilde{C}(f)$ and $2T\tilde{R}'(f)$, was less than that in the absence of the constant opposing torque [Figs. 3(c) and 3(f)].

Next, we focus on the energetics. ATP hydrolysis and mechanical motion are known to be tightly coupled in the hydrolytic reactions of $F_1$-ATPase; an ATP hydrolysis triggers a step of 120° rotation [4,5]. Therefore, the number of steps, or the number of ATP consumptions, per unit time is $3v_s$. To clarify the energy balance, we compared the heat and work per a step with the free energy consumption of an ATP hydrolysis. The heat per a step is equivalent to $Q_{\rm rot} \equiv J/3v_s$, where $J$ is the heat per unit time calculated using (1). Note that the integral in (1) corresponds to twice of the area between $\tilde{C}(f)$ and $2T\tilde{R}'(f)$ shaded in Fig. 3. We limited the integration in the range up to 300 Hz to avoid the systematic noise in the high frequency region. $\Gamma$ was obtained by taking the average of $\tilde{C}(f)$ around 300 Hz by assuming the FRR in high frequency regions as $\tilde{C}(f) = 2T/\Gamma$. The work performed against the external load $N$ during a step is $W = N \times 120°$. On the other hand, the free energy consumption of an ATP hydrolysis is $\Delta\mu \simeq \Delta\mu° + T\ln([\mathrm{ATP}]/[\mathrm{ADP}][\mathrm{P_i}])$, where the standard free energy difference $\Delta\mu°$ was calculated on the basis of the literature [25–29]. In Fig. 4, we plot $Q_{\rm rot}$, $W$ and $\Delta\mu$, where $Q_{\rm rot}$ is shown separately: the contribution from the steady motion $Q_s \equiv \Gamma v_s^2/3v_s$ and that from nonequilibrium fluctuations $Q_v \equiv \Gamma \int df[\tilde{C}(f) - 2T\tilde{R}'(f)]/3v_s$. We found an energy balance relation $W + Q_{\rm rot} \simeq \Delta\mu$ under all the conditions we examined. When we increased ATP and ADP concentration together while $\Delta\mu$ was held to be constant [Fig. 4(i–iii)], $v_s$ and accordingly $Q_s$ increased, and $Q_v$ decreased. This is because the $\gamma$ shaft rotates rapidly and smoothly at high ATP concentrations with short waiting time for the ATP binding. Under an external load, $F_1$ performs work against the load. Although $Q_s$ and $Q_v$ decreased simultaneously under an external load [Fig. 4(iv)], the sum $W + Q_{\rm rot}$ was almost equal to $\Delta\mu$. At a constant ATP concentration and different $\Delta\mu$ [Fig. 4(ii, v)], $v_s$ and accordingly $Q_s$ were almost the same, but $Q_v$ increased together with $\Delta\mu$. In addition, the Stokes efficiency defined as the ratio $Q_s/(\Delta\mu - W)$ was always less than unity, as expected [25,30] (Fig. 4). High Stokes efficiency implies that the driving force of a motor is nearly constant.

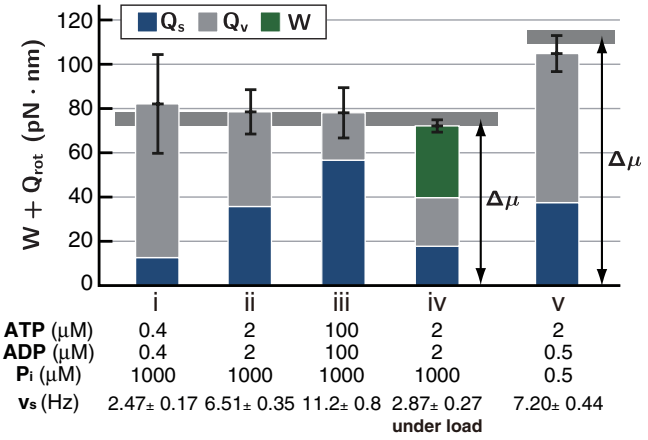


FIG. 4 (color online). Amount of heat dissipation per a step $Q_{\rm rot}$, the work on an external load per a step $W$, and the free energy difference of an ATP hydrolysis $\Delta\mu$. $Q_{\rm rot} = Q_s + Q_v$ is separately plotted: the contribution from the steady motion $Q_s$ and that from nonequilibrium fluctuations $Q_v$. The horizontal thick lines indicate $\Delta\mu$ calculated on the basis of $\Delta\mu°$ reported in the literature [25–29]. Since $\Delta\mu°$ are different in the literature, the error of the estimation of $\Delta\mu$ is indicated as the thickness of the line: 72.4–78.4 pN nm (i–iv) and 109–115 pN nm (v). In (i–iv), the ratio $[\mathrm{ATP}]/[\mathrm{ADP}][\mathrm{P_i}]$ and accordingly $\Delta\mu$ are held to be constant except for a minor difference due to changes in the ionic strength, concentration of free $Mg^{2+}$, etc. Error bars indicate the standard deviations. Number of samples are (i) 15, (ii) 8, (iii) 7, (iV) 5, and (V) 7, respectively.

The relation $W + Q_{\mathrm{rot}} \simeq \Delta\mu$ seems to imply that $F_1$-ATPase focuses all of the free energy consumption on the rotational degree of freedom despite that there are multiple degrees of freedom. However, we need to be careful since $Q_{\mathrm{rot}}$ is nothing but a heat dissipation; the heat is not necessarily limited by the free energy change $\Delta\mu$ and can actually exceed $\Delta\mu$ [30]. Nevertheless, our results suggest that $F_1$-ATPase works at an efficiency of nearly 100% as follows (see also [25]). Since we attached a large probe particle to the $\gamma$ shaft with a relatively soft elastic linker, the time scale of the $\gamma$ shaft's motion is much faster than that of the particle. As the $\gamma$ shaft rotates, the probe does not rotate immediately due to the friction. Therefore, work performed by the $\gamma$ shaft on the linker is stored as an elastic energy of the linker, which then dissipates through the delayed motion of the probe as $Q_{\mathrm{rot}}$ or is used to oppose the external load if subjected to the external load. Since the work on the linker is against a conservative elastic force and cannot exceed $\Delta\mu$, $W + Q_{\mathrm{rot}}$ is limited by $\Delta\mu$. Thus, $W + Q_{\mathrm{rot}} \sim \Delta\mu$ suggests that the $F_1$ motor works at an efficiency of nearly 100%. Note that $W + Q_{\mathrm{rot}}$ is an extractable work by coupling an appropriate system to the probe. On the other hand, if the time scale of the probe is faster than that of the $\gamma$ shaft by attaching sufficiently small probes with a stiff linker, it is expected that the probe follows the motion of the $\gamma$ shaft without delay. If this is the case, in addition to $\Delta\mu$, there may be inextractable heat absorption or dissipation through the rigid complex of the probe and shaft. In our system, with a large probe, it is possible that there is such an additional heat flow through the rotation of the $\gamma$ shaft. However, this heat does not conduct to the probe and is directly exchanged between the shaft and surrounding medium. Thus, by insulating the probe from the $\gamma$ shaft, we measured only the extractable work of $F_1$-ATPase and found that it works at an efficiency of nearly 100%.

In summary, we measured the violation of the fluctuation response relation of $F_1$-ATPase at a single molecule level. From the extent of this violation, we calculated the thermodynamic quantities of the probe using a nonequilibrium equality and found that $F_1$-ATPase works at an efficiency of nearly 100% under a large variety of conditions. The free energy conversion at 100% efficiency does not contradict the thermodynamic laws, yet it is surprising that such highly efficient machinery exists and is actually working in cells. It is also worth noting that $F_1$-ATPase adapts to a large variety of conditions to retain this efficiency. Since the rotation of the $\gamma$ shaft is the sole handle to transmit energy between $F_1$ motor and $F_0$ motor in cells, this high efficiency might have been developed for the efficient coupling of ATP hydrolysis or synthesis and proton transport during a long evolutionary process. Including this possibility, detailed mechanism and meaning of such highly efficient energy transduction remain subjects for future study.

We appreciate critical discussions with Masaki Sano, Takahiro Harada, Makito Miyazaki, Felix Ritort, Ken Sekimoto, Shigeru Sugiyama, and Kazuhiko Kinosita, Jr. This work was supported by Japan Science and Technology Agency (JST) and Grant-in-Aid for Scientific Research on Priority Areas, 18074001, 17049015, 19037022, 18031033 (to E. M.), and 21740291 (to S. T.).

*emuneyuk@phys.chuo-u.ac.jp

[1] P. D. Boyer, Biochim. Biophys. Acta **1140**, 215 (1993).
[2] J. P. Abrahams, A. G. W. Leslie, R. Lutter, and J. E. Walker, Nature (London) **370**, 621 (1994).
[3] H. Noji, R. Yasuda, M. Yoshida, and K. Kinosita, Jr., Nature (London) **386**, 299 (1997).
[4] R. Yasuda, H. Noji, K. Kinosita, Jr., and M. Yoshida, Cell **93**, 1117 (1998).
[5] Y. Rondelez *et al.*, Nature (London) **433**, 773 (2005).
[6] K. Adachi *et al.*, Cell **130**, 309 (2007).
[7] E. Muneyuki *et al.*, Biophys. J. **92**, 1806 (2007).
[8] T. Harada and S.-I. Sasa, Phys. Rev. Lett. **95**, 130602 (2005).
[9] T. Harada and S.-I. Sasa, Phys. Rev. E **73**, 026131 (2006).
[10] J. M. Deutsch and O. Narayan, Phys. Rev. E **74**, 026112 (2006).
[11] M. Washizu *et al.*, IEEE Trans. Ind. Appl. **29**, 286 (1993).
[12] R. M. Berry, L. Turner, and H. C. Berg, Biophys. J. **69**, 280 (1995).
[13] T. Watanabe-Nakayama *et al.*, Biochem. Biophys. Res. Commun. **366**, 951 (2008).
[14] C. Bustamante, J. Liphardt, and F. Ritort, Phys. Today **58**, No. 7, 43 (2005).
[15] V. Blickle *et al.*, Phys. Rev. Lett. **96**, 070603 (2006).
[16] K. Sekimoto, J. Phys. Soc. Jpn. **66**, 1234 (1997).
[17] K. Sekimoto, *Stochastic Energetics (Lecture Notes in Physics)* (Springer, Berlin, 2010).
[18] S. Toyabe *et al.*, Phys. Rev. E **75**, 011122 (2007).
[19] S. Toyabe and M. Sano, Phys. Rev. E **77**, 041403 (2008).
[20] R. Kubo, M. Toda, and N. Hashitsume, *Statsitical Physics II* (Springer, Berlin, 1991), 2nd ed..
[21] D. Mizuno, C. Tardin, C. F. Schmidt, and F. C. Mackintosh, Science **315**, 370 (2007).
[22] T. Speck and U. Seifert, Europhys. Lett. **74**, 391 (2006).
[23] V. Blickle *et al.*, Phys. Rev. Lett. **98**, 210601 (2007).
[24] J. R. Gomez-Solano *et al.*, Phys. Rev. Lett. **103**, 040601 (2009).
[25] See supplementary material at http://link.aps.org/supplemental/10.1103/PhysRevLett.104.198103.
[26] J. Rosing and E. C. Slater, Biochim. Biophys. Acta **267**, 275 (1972).
[27] R. W. Guynn and R. L. Veech, J. Biol. Chem. **248**, 6966 (1973).
[28] O. Pänke and B. Rumberg, Biochim. Biophys. Acta **1322**, 183 (1997).
[29] K. Krab and J. van Wezel, Biochim. Biophys. Acta **1098**, 172 (1992).
[30] H. Wang and G. Oster, Europhys. Lett. **57**, 134 (2002).